Graefes Arch Clin Exp Ophthalmol (2008) 246:803–810
DOI 10.1007/s00417-007-0749-4

RETINAL DISORDERS

Are low inflammatory reactions involved in exudative age-related macular degeneration?

Morphological and immunhistochemical analysis of AMD associated with basal deposits

A. Lommatzsch · P. Hermans · K. D. Müller · N. Bornfeld · A. C. Bird · D. Pauleikhoff

Received: 16 May 2007 / Revised: 31 October 2007 / Accepted: 29 November 2007 / Published online: 15 April 2008

Abstract
Purpose Basal laminar and linear deposits (BLD) are associated with the development of choroidal neovascularization (CNV). Therefore, analysis of BLD composition may provide further information concerning the pathogenesis of BLD and CNV in age-related macular degeneration (AMD).
Methods BLD in 25 specimens of surgically removed CNV were examined, using histochemical and immunohistochemical methods, for extracellular matrix proteins and their modulating enzymes, and for cell markers and proteins involved in inflammatory processes. In addition, ultrastructural electron microscopic analysis (EM) was performed.
Results The chemical and structural composition of all the BLD was similar. Only the inner aspect of the BLD contained laminin and collagen IV, which corresponded to a new RPE basal lamina upon EM analysis. The extracellular matrix protein predominantly found in all layers of BLD was vitronectin, which was seen as a homogeneous material within the BLD upon EM analysis. The metalloproteinases MMP-2 and MMP-9 could only be detected in the inner aspect, while MMP-7 and TIMP-3 were observed predominantly in the outer aspect of BLD. In this area, staining for phospholipids and less intensely for neutral lipids was also visible. The labelling of complement complexes C3 and C5b-9 was intensely positive, and vascular endothelial growth factor (VEGF) was detected in all BLDs.
Conclusions Diffuse deposits such as BLD appear consistently with the development of CNV in AMD. They consist of extracellular matrix components and predominantly vitronectin. However, activated complement and VEGF could also be detected. The results of the current study may support the hypothesis that inflammatory processes are involved in the pathogenesis of BLD and CNV in AMD.

Keywords Age-related macular degeneration · AMD pathogenesis · Basal laminar and linear deposits · Inflammation · Histology

A. Lommatzsch · P. Hermans · D. Pauleikhoff
Department of Ophthalmology and Ophtha-Lab,
St. Franziskus Hospital Münster,
Münster, Germany

K. D. Müller
Department of Microbiology, University of Essen-Duisburg,
Essen, Germany

P. Hermans · N. Bornfeld
Department of Ophthalmology, University of Essen-Duisburg,
Essen, Germany

A. C. Bird
Moorfields Eye Hospital,
London, UK

A. Lommatzsch (✉)
Department of Ophthalmology, St. Franziskus Hospital,
Hohenzollernring 74,
48145 Münster, Germany
e-mail: Albrecht.Lommatzsch@web.de

Introduction

Exudative age-related macular degeneration (AMD) is the leading cause of legal blindness in developed countries [8, 9, 27]. Choroidal neovascularization (CNV) represents the most serious complication of AMD, and results in loss of vision. Clinically, CNV is often associated with focal deposits in Bruch's membrane, known as drusen [12, 24]. In addition, histological studies of donor eyes and AMD specimens revealed the presence of diffuse basal laminar and linear deposits (BLD) between the cytoplasmic and

basal membrane of the retinal pigment epithelium (RPE) to be highly significantly associated with CNV development [18, 23, 29, 34]. The formation of extracellular deposits that are localized as drusen and diffuse as in BLD is thought to be a consequence of RPE dysfunction [3, 50], but a chronic inflammatory process in Bruch's membrane and choroid may be involved [3, 19, 20, 25]. The presence of activated complement within drusen, and the recent molecular genetic observation of an association between specific complement factor H polymorphism and the development of AMD, support this hypothesis [16, 21, 22, 28]. Despite intensive efforts to determine the composition of the material of drusen, only limited information about the composition of BLD is available to date, especially with respect to inflammatory processes [29, 35].

As a close correlation between BLD and CNV has been reported, the aim of the present study was to analyze more specifically the composition of BLD. These investigations may provide new information about the influence of inflammatory processes in the pathogenesis of BLD and CNV in AMD.

Material and methods

During macular translocation surgery, 25 CNV specimens were removed and collected from ten men and 15 women with AMD, age ranging between 67 and 97 years (mean 78 years). These specimens were stored in liquid nitrogen at −80°C. The study was conducted in accordance with the Declaration of Helsinki, and informed consent was obtained from the patients after explaining the nature of the study. The local ethics committee approved the research.

For histochemical and immunohistochemical analysis, the specimens were embedded in optimal freezing compound (OCT), and cryosections (5 μm) were obtained with a cryostat at −25°C- −30°C. Slices were mounted on Poly-L-Lysine coated slides. The slides not stained immediately were stored at −20°C.

Histochemistry

For lipid analysis, Oil red O staining was used to demonstrate the presence of neutral lipids, and acetone-sudan black B for the presence of phospholipids, as previously described [7, 37–39]. Amyloid was detected with Congo red. For PAS and alcian blue staining for the detection of heparan sulfates and collagen, the protocol described by Scott and Dorling was used [46]. Masson trichrome staining was carried out as follows. Slides were thawed, dried and preserved in Bouin's solution for 1 h at 56°C. After cooling and rinsing under running water, the slides were washed in distilled water. The slides were then placed in Weigert's iron hematoxylin solution for 10 min to stain the nuclei, and then rinsed under running water and washed in distilled water. This was followed by staining with Biebrich Scarlet for 10 min. After rinsing the specimens in distilled water, staining procedures using molybdatophosphoric acid hydrate/ tungstophosphric acid hydrate solution for 7 to 10 min and then anilin blue for 10 min were perfomed. Finally, the slides were rinsed in distilled water, dehydrated in an increasing ethanol line and covered.

Transmission electron microscopy

From five of the specimens (67 y to 75 y), one half of the sample was fixed and stored at 4°C in 2.5% glutaraldehyde in 0.1 M sodium cacodylate buffer, ph 7.4. Then they were washed in 0.1 M sodium cacodylate buffer and fixed in 4% osmium tetroxide in 0.1 M sodium cacodylate buffer, pH 7.4, for 30 min. After an additional washing with 0.1 M sodium cacodylate buffer, the specimens were dehydrated stepwise in acetone at various concentrations (30%, 50%, 70% overnight, 80%, 90%, 100%, each 3×15 min) at room temperature. Subsequently, the specimens were immersed in Durcupan-ACM (Fluka) acetone 1:1 twice for 30 min and Durcupan for 1 hour. The final step involved embedding the samples in moulds for flat mounts (Agar Scientific). For this they were immersed in fresh Durcupan for 6 h at 40°C and then polymerized for 60 hours at 60°C. Semi-thin sections (~1 μm) were cut with glass knifes and stained with 1% toluidine blue-borax solution (1:1) to confirm the correct orientation of the specimen. These sections were used to guide trimming of ultrathin sections. Ultrathin sections (~0.6 μm) from each specimen were prepared on an Ultramicrotome (Ultracut E, Reichert-Jung) using a diamond knife (Delaware DDK) and then transferred to polyvinyl formal-coated (Formvar) copper slot grids. The grids were contrasted as described by Reynolds [41]. Briefly, the grids were stained with 10% uranylacetate in 50% ethanol for 15 min and, after rinsing in distilled water eight times, the grids were stained with 1% lead citrate for 2 min; an additional eight rinses followed. The specimens were examined under a Zeiss EM 900 electron microscope at a magnification of 3400× to 20000×.

Immunohistochemistry

For immunohistochemistry the avidin-biotin complex (ABC) method was used. The frozen slides were air dried and fixed in acetone for 10 minutes at room temperature. Sections were rehydrated in phosphate-buffered saline (PBS) and incubated for 20 minutes in blocking solution (5% normal sera rabbit or goat—depending on the 2nd antibody—in PBS containing 5% fetal calf serum). The sections were incubated, depending on individual experi-

Table 1 Primary antibodies

Antibody	Clone	Source	Product Number	Supplier
Laminin	LAM-89	Mouse monoclonal	L-8271	Sigma, St. Louis, MO, USA
Collagen IV	CIV 22	Mouse monoclonal	M 0785 Lot 020	Dako, Denmark
Collagen VI		Rabbit polyclonal	AB 7821	Chemicon, Temecula, CA, USA
Fibronectin		Rabbit polyclonal	A 245 Lot 117	Dako
Vitronectin		Mouse monoclonal	MAB 1945	Chemicon
MMP-2		Goat polyclonal	Sc-6838	Santa Cruz Biotechnology, Santa Cruz, CA, USA
MMP-7		Goat polyclonal	Sc-8832	Santa Cruz Biotechnology
MMP-9		Goat polyclonal	Sc-6841	Santa Cruz Biotechnology
TIMP-2		Goat polyclonal	Sc-6835	Santa Cruz Biotechnology
TIMP-3		Goat polyclonal	Sc-9906	Santa Cruz Biotechnology
C-3	HAV 3-4	Mouse monoclonal	M 0836 Lot 040	Dako
C5b-9	AE 11	Mouse monoclonal	M 0777 Lot 030	Dako
CD14	TÜK 4	Mouse monoclonal	M 0825 Lot 036	Dako
CD68	EBM 11	Mouse monoclonal	M 0718 Lot 059	Dako
HLA-DR, beta chain	DK22	Mouse monoclonal	M 0704 Lot 077	Dako
VEGF		Mouse monoclonal	555036	BD Pharmingen, San Diego, CA, USA
IgM		Rabbit	F 0203 Lot 050	Dako
IgA		Rabbit	F 0204 Lot 051	Dako
IgG		Rabbit	F 0202 Lot 111	Dako
IgE		Rabbit	F 0352 Lot 098	Dako

ence with primary unconjugated antibodies, between 20 to 60 minutes or overnight at room temperature in a wet chamber (for a summary of the antibodies used, see Table 1). After washing with PBS three times for 5 minutes each time, endogenous peroxidase activity was blocked by incubation in 3% hydrogen peroxide for 5 minutes. After washing three times for 5 minutes with PBS, the specimens were incubated with a second biotinylated antibody (Rb × Ms or Gt × Rb, Dako, Denmark) for 20 to 60 minutes, and then washed three times for 5 minutes with PBS. The specimens were then incubated with a horseradish peroxidase streptavidin complex (Dako, Denmark) for 20 minutes, and washed three times for 5 minutes with PBS; the staining reaction was processed by adding the substrate (3-amino-9-ethylcarbazol solution). The reaction was observed under the microscope and stopped after 10 to 20 minutes by fixing the slices in 4% formalin in acetate buffer. They were then incubated in 1% acetic acid and counterstained with hematoxylin Gill No. 3 (Sigma Diagnostics, St. Louis, MO, USA) for 10 to 15 seconds. The slides were washed in water and mounted with aquatex (Merck, Darmstadt, Germany). This method was used for the extracellular matrix protein antibodies laminin (monoclonal anti-laminin, Sigma Immunochemicals, epitope not exactly characterised), collagen IV (monoclonal Mouse anti Human antibodies (Ms × Hu) from Dako, Denmark,

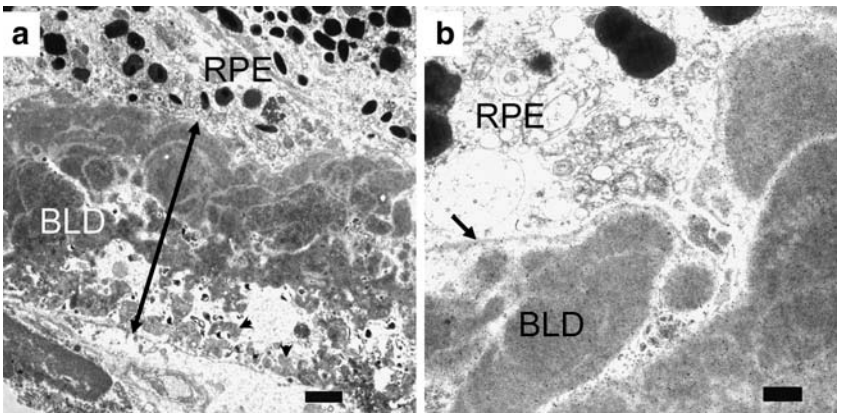

Fig. 1 TEM of BLD. At 3000× magnification the extension of BLD (*double arrow*) is shown in **a**; scale bar=2 μm. The internal aspect of the BLD has a homogeneous, cloudy-like appearance, while the external part contains vesicles and long spacing collagen (*arrowheads*). At a higher magnification (20000×, scale bar=0.6 μm) a basement membrane like structure (*arrow*) was observed (**b**) between retinal pigment epithelial cells (RPE) and BLD. No further fine structure was observed in the homogeneous material of BLD showing the same electron density as basement membrane

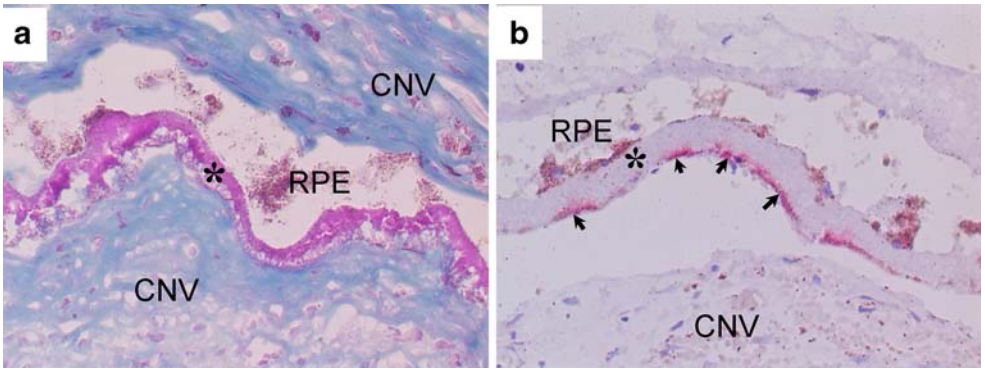

Fig. 2 Histochemical staining of frozen sections. **a** BLD (*star*) stained pink with alcian blue, indicating the presence of heparan sulfate. **b** Positive Oil red O staining in the external part of BLD (*arrowheads*), indicating the presence of neutral lipids. Original magnification **a** and **b**: 200×

epitope not exactly characterised) and collagen VI (polyclonal Rb × collagen VI antibody from Chemicon, Temecula, CA, USA), fibronectin (Rb × Hu, Dako, Denmark) and vitronectin (monoclonal Ms × Hu vitronectin antibody from Chemicon, Table 1), and for the extracellular matrix-modulating metalloproteinases MMP-2, MMP-7, MMP-9 and their inhibitors TIMP-2 and TIMP-3 (all goat polyclonal antibodies, Santa Cruz Biotechnology, Santa Cruz, USA, Table 1). The distribution of C3 and C5b-9 as components of the complement system was analyzed. Additionally, the occurrence of the macrophage-markers CD14 and CD68 was examined (all antibodies, see Table 1). The monoclonal Ms × Hu HLA-DR antibody recognizes the beta chain and was purchased from DAKO, Denmark, the monoclonal mouse anti-human vascular endothelial growth factor (VEGF) antibody from BD PharMingen (San Diego, CA, USA, Table 1).

In order to investigate the possible presence of immunoglobulins, IgM, IgA, IgG, IgE fluorescein thiocyanate (FITC) conjugated Ms x Hu Ig's (Dako, Table 1) were used. Slides were air dried, rehydrated in PBS three times for 5 minutes, and incubated with the FITC-conjugated antibody for 20 minutes in a dark wet chamber. After rinsing in PBS the slides were mounted with Fluoprep (bioMérieux, Marcy l'Etoile, France). Negative controls were prepared by omitting the first antibody.

To describe the results clearly, we use the term "inner aspect of BLD" for the position next to RPE and the term "outer aspect of BLD" for positions next to Bruch's membrane.

As a marker of reactive oxygen species mediated protein oxidation and oxidative stress, protein carbonyls were detected by the DNPH method using Oxyblot Protein Oxidation Detection Kit (Qbiogene, Heidelberg, Germany). Carbonyl residues were detected by reaction with 2,4-dinitrophenylhydrazine (DNPH) generating dinitrophenylhydrazones. The visualization was processesed with an anti-dinitrophenylhydrazone antibody followed by the immunohistochemical ABC method. Immunoreactivity was resolved with horseradish peroxidase-aminoethylcarbazole, which produces a magenta reaction product. Two different negative controls were performed using a control derivatization solution instead of DNPH solution or buffer samples to replace the primary antibody.

Results

General appearance

The excised CNV membranes contained predominantly fibrovascular tissue and RPE cells as monolayer. Between the RPE and the fibrovascular tissue, the material showed a cell-free layer of extracellular material. These BLD were seen in all specimens.

Electron microscopy

The results of the five investigated BLD were very similar. Ultrastructural analysis of the specimens showed thick BLD at the basal side of the RPE cells, with a heterogeneous composition. At the inner aspect of BLD, a fine homogeneous electron-dense line was visible. Furthermore, homogeneous accumulations with the same electron density were found in the inner aspect of BLD. The outer aspect of BLD was less homogeneous, and contained several droplets and

Table 2 Lipids and potential extracellular components in BLDs

	BLD positive
Neutral lipids	25/25
Polar lipids	25/25
Oxidized proteins	1/25
Amyloid beta	0/25

Table 3 Extracellular matrix proteins in BLDs

	BLD positive
Laminin	25/25
Collagen IV	22/25
Fibronectin	0/25
Vitronectin	25/25

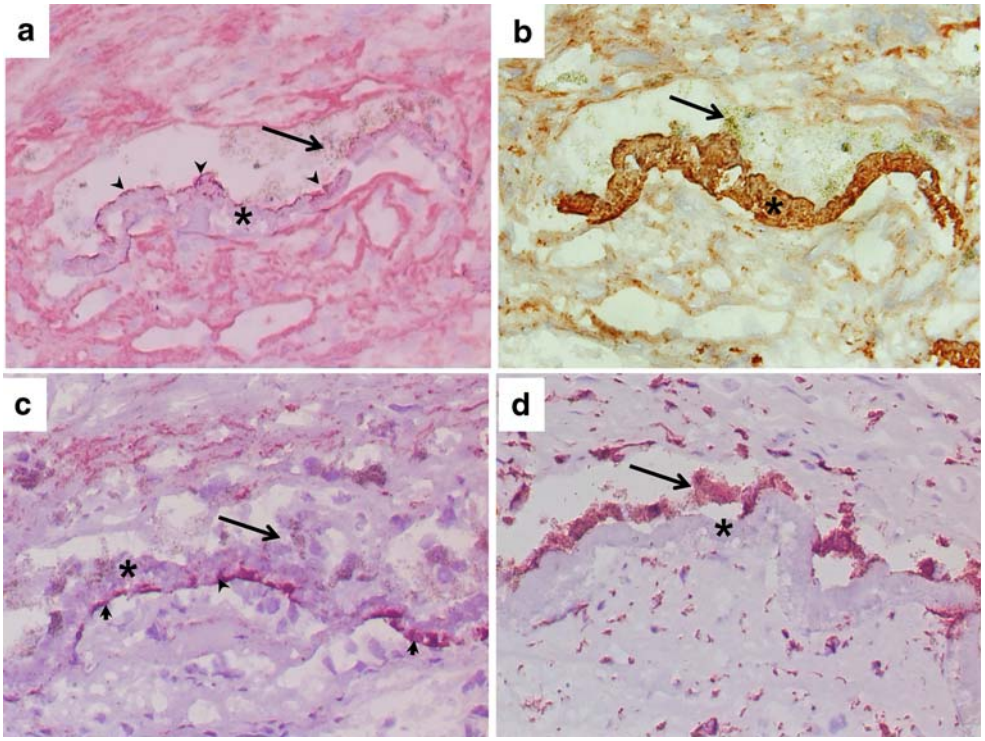

Fig. 3 Immunostaining of frozen sections of BLD for extracellular matrix proteins and inflammatory markers (original magnification **a**–**d**, 200×). **a** BLD (*star*) was immunoreactive for laminin at the internal border of BLD (*arrowheads*), indicating basement membrane production by retinal pigment epithelium cells (*arrow*). **b** BLD (*star*) was strongly immunoreactive for vitronectin (*arrow* RPE cells). **c** The external part of BLD (*star*) was immunoreactive for the complement factor c5b-9 (membrane-attacking complex) (*arrowheads*), (*arrow* RPE cells). **d** The macrophage marker CD68 reacted with the retinal pigment epithelium (*arrow*) and cells at the external border of BLD

vesicles of different size and varying electron density, as well as long spacing material (LSC) (Fig. 1a,b).

General stainings and lipids

PAS (not shown) and alcian blue (Fig. 2a) stained BLD bright pink, and with Masson trichrome (not shown) BLD stained blue and violet. The outer aspect of BLD stained for phospholipids and less intensely for neutral lipids (Fig. 2b).

ECM proteins and regulators

In immunohistological analysis, laminin and collagen IV, but not collagen VI, were detected in the inner aspect of BLD. Vitronectin was visible throughout BLD, but fibronectin seems to be absent in BLD (Tables 2 and 3, Fig. 3a,b).

The ECM-modulating metalloproteinases MMP-2 and MMP-9 were visible at the inner aspect of BLD, whereas MMP-7 was visibly dispersed both in BLD and the inhibitors TIMP-2 and TIMP-3, which were found more often in the outer aspect of the BLDs (Table 4, Fig. 4a–c).

Inflammatory processes

In addition, the presence of activated complement complexes C3 and C5b-9 was readily detected at the outer aspect of BLD. CD68-positive cells were found at the outer aspect of BLD in four of 25 investigated specimens (Fig. 3c,d), but neither CD14- nor HLA-DR-positive cells were seen in BLD. Immunoglobulins were not detected in any BLD either. (Table 5)

Growth factor

The investigated growth factor VEGF was detected at the basal surface of the RPE in all samples (Fig. 4d).

Discussion

Linear thickening in the inner aspect of Bruch's membrane was first described by Sarks et al. [42] as an accumulation of amorphous material. This material was initially termed basal linear deposits [35, 43, 44]; however, this term was later replaced by BLD [42, 43], which describes material deposited with age between the outer plasma membrane and the basement membrane of RPE cells. Within the BLD, extracellular matrix proteins were detected [35, 44], which was confirmed by PAS, alcian blue, and Masson trichrome

Table 4 Metalloproteinases (MMP) and their inhibitors (TIMP) in BLDs

	BLD positive
MMP-2	0/25
MMP-7	15/25
MMP-9	17/25
TIMP-2	13/25
TIMP-3	25/25

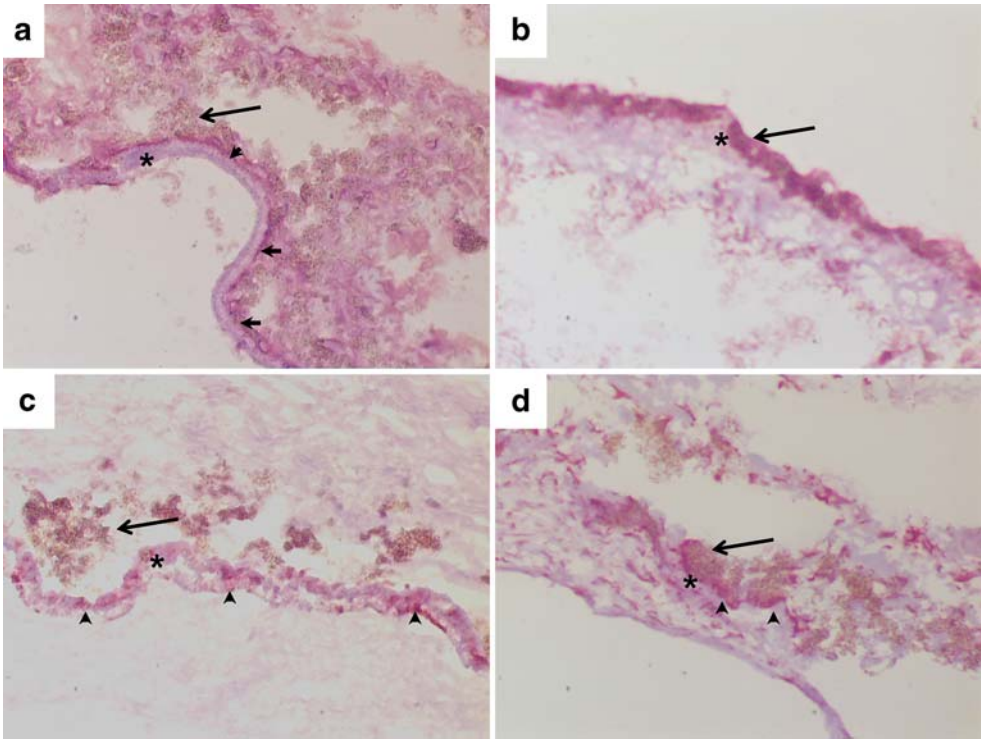

Fig. 4 Immunostaining of frozen sections of BLD (*stars*) for MMP-2, MMP-9, TIMP-3, and VEGF(Original magnification **a**–**d**, 200×, *arrow* at the RPE). **a** Immunoreactivity for MMP-2 (*arrowheads*) was visible at the basolateral surface of RPE at the internal aspect of BLD *(star)*. **b** MMP-9 stained RPE and the internal aspect of BLD *(star)*, too. **c** TIMP-3 antibody was detectable in BLD *(star),* with continuous staining in the external part of BLD (*arrowheads*). **d** Immunoreactivity for VEGF antibody (*arrowheads*) was seen at the basolateral surface of the RPE at the internal aspect of BLD *(star),* similar to the appearance of MMP-2

staining for the basement membrane ground matrix components heparan sulfate and collagen. Our data showed that oil red O staining could be found at the outer aspect of the BlamD, and this was similar to the finding of a previous study showing that esterified cholesterol was present at the same site [45].

In addition, laminin and collagen IV were demonstrated within the inner aspect of BLD. This is in contrast to the basement membrane of the RPE in age-matched macular specimens, where no immunoreactivity was detected [22]. This immunoreactivity of ECM proteins may therefore be an indicator for a newly formed RPE basement membrane. The results of the EM analysis showing a basement membrane-like structure immediately adjacent to the RPE cells support this interpretation.

EM analysis also demonstrated the homogeneous inner structure of BLD, in which vitronectin was a prominent component based on the immunohistochemical study. This ECM protein is present in many human structures as an important response for activated complement. Indeed, fibronectin and vibronectin have become highly relevant for understanding the pathogenesis not only of vascular eye diseases but also of coronary artery diseases and Alzheimer's disease [1, 17].

In the outer aspect of BLD, we found a strong staining for phospholipids and to a lesser extent for neutral lipids, while no oxidatively damaged proteins or amyloid ß were detected, unlike Alzheimer's disease plaques [4]. The histochemical results indicate that the vesicles and droplets seen by TEM are in part lipid droplets. It is supposed that the LSC seen by TEM in the outer aspect of BLD is a type of collagen VI [30]. However, the present and earlier studies have failed to confirm immunologically that collagen type VI is present in LSC [14, 36, 49].

In accord with the findings of other authors, the present study also shows that the ECM-modulating metalloproteinases MMP-2 and MMP-9 are present at the basal RPE cell surface [31, 33, 48]. In contrast to the results from a study of Kadonosono et al. [26], we found only the vitronectin-degrading MMP-7 in 60% of the specimens. In addition, the immunoreactivity was patchier throughout the BLD. Furthermore, the degrading enzymes MMP-2 and MMP-9 are restricted to the RPE basolateral surface. TIMP-2 and TIMP-3 are predominantly detectable in the outer aspect of BLD. Kamei and Hollyfield [6] found an increased expression of TIMP-3 with age in Bruch's membrane. Consistent with that finding, our staining results demonstrated that TIMP-3 was also detected in BLD. This

Table 5 Macrophages, immunoglobulins and proteins of the complement cascade in BLDs

	BLD positive
CD 68	0/25
CD 14	0/25
HLA-DR	0/25
IgG	0/25
IgM	0/25
C3	25/25
C5b-9	25/25

might imply an imbalance between synthesis, degradation, and inhibition of degradation of the ECM proteins that was observed in Sorsby's fundus dystrophy [10].

In all specimens, complement components C3 and C5b-9 (membrane attack complex, MAC) were shown throughout BLD. In contrast, immunoglobulins were not detected. This negative result might be due to the lower sensitivity of direct immunofluorescence. These results may suggest complement activation in the absence of immunoglobulin. Recently, an association was shown between a genetic polymorphism of the complement factor H (CFH) and AMD [16, 21, 22, 28], implying that some kind of dysregulation of complement activation plays a role in the pathogenesis of AMD. The MAC may threaten survival of the overlying RPE cells, and the observed deposition of vitronectin in BLD may be protective [15, 20]. The histological appearance is very similar to that in the glomeruli from patients affected by type II membranoproliferative glomerulonephritis, which is also associated with mutations in the CFH gene. The observation that dysregulation of the complement cascade caused by failure of complement factor H leads to uncontrolled C3 activation [2, 5, 40] also supports this hypothesis.

Macrophages may be involved in this chronic inflammatory process. Cui et al. [11] have shown that macrophages are involved only in very early phases of CNV development. The fact that we investigated established CNV complexes may explain the absence of macrophages in our study. The antibody we used reacts with the lysosomal compartment of phagocytosing cells; therefore, the RPE shows strong immunoreactivity. As a result, we cannot exclude the possibility that the positive reaction with CD68 at the basal border of BLD involves remnants of RPE cells.

The presence of VEGF at the basolateral side of the RPE indicates a high expression or accumulation of this growth factor, which is known to have angiogenic properties and is involved in the pathogenesis of CNV [47].

Summary

Diffuse deposits, such as BLD, appear consistently when CNV develops secondary to AMD [23, 29]. They are composed of new basement membrane material and excessive extracellular matrix proteins, predominantly vitronectin. In addition, extracellular matrix-modulating metalloproteinases such as MMP-2, MMP-7, and MMP-9 and their inhibitors TIMP-2 and TIMP-3 were present. However, activated complement and VEGF were also detected. The results of our present analysis support the hypothesis that inflammatory processes are involved in the pathogenesis of BLD and CNV in AMD.

Acknowledgements Supported by the German science foundation DFG (Pa357/5-1, Pa357/5-2) and the Voltmann Foundation.

References

1. Aksenov MY, Aksenova MV, Butterfield DA, Geddes JW, Markesbery WR (2001) Protein oxidation in the brain in Alzheimer's disease. Neuroscience 103:373–383
2. Alexander JJ, Pickering MC, Haas M, Osawe I, Quigg RJ (2005) Complement factor h limits immune complex deposition and prevents inflammation and scarring in glomeruli of mice with chronic serum sickness. J Am Soc Nephrol 16:52–57
3. Anderson DH, Mullins RF, Hageman GS, Johnson LV (2002) A role for local inflammation in the formation of drusen in the aging eye. Am J Ophthalmol 134:411–431
4. Anderson DH, Talaga KC, Rivest AJ, Barron E, Hageman GS, Johnson LV (2004) Characterization of ß amyloid assemblies in drusen: the deposits associated with aging and age-related macular degeneration. Exp Eye Res 78:243–256
5. Appel GB, Cook T, Hageman G, Jennette JC, Kashgarian M, Kirschfink M, Lambris JD, Lanning L, Lutz HU, Meri S, Rose NR, Salant Dj, Sehti, Smith RJH, Smoyer W, Tully HF, Tully Sp, Walker P, Welsh M, Würzner R, Zipfel PF (2005) Membranoproliferative glomerulonephritis type II (dense deposit disease): an update. J Am Soc Nephrol 16:1392–1403
6. Kamei M, Hollyfield JG (1999) TIMP-3 in Bruch's membrane: changes during aging and in age-related macular degeneration. Invest Ophthalmol Vis Sci 40:2367–2375
7. Bayliss High O (1984) Lipid histochemistry (Royal Microscopical Society Microscopy Handbooks Number 6). Oxford University Press, Oxford
8. Bird AC, Marshall J (1986) Retinal pigment epithelial detachments in the elderly. Trans Ophthalmol Soc U K 105:674–682
9. Bressler NM, Bressler SB, West SK, Fine SL, Taylor HR (1989) The grading and prevalence of macular degeneration in Chesapeake Bay waterman. Arch Ophthalmol 107:847–852
10. Capon MRC, Marshall J, Krafft JI, Alexander RA, Hiscott PS, Bird AC (1989) Sorsby's fundus dystrophy. A light and electron microscopic study. Ophthalmology 96:1769–1777
11. Cui JZ, Rimura H, Spee C, Thumann G, Hinton DR, Ryan SJ (2000) Natural history of choroidal neovascularisation induced by vascular endothelial growth factor in the primate. Graefes Arch Clin Exp Opthalmol 238:326–333
12. Curcio CA, Millican CL (1999) Basal linear deposit and large drusen are specific for early age-related maculopathy. Arch Ophthalmol 117:329–339
13. Curcio CA, Millican CL, Bailey T, Kruth HS (2001) Accumulation of cholesterol with age in human Bruch's membrane. Invest Ophthalmol Vis Sci 42:265–274
14. Das A, Frank RN, Zhang NL, Turczyn TJ (1990) Ultrastructural localization of extracellular matrix components in human retinal vessels and Bruch's membrane. Arch Ophthalmol 108: 421–429
15. de Boer HC, Preissner KT, Bouma BN, de Groot PG (1992) Binding of vitronectin-thrombin-antithrombin III complex to human endothelial cells is mediated by the heparin binding site of vitronectin. J Biol Chem 267:2264–2268
16. Edwards AO, Ritter III R, Abel KJ, Manning A, Panhuysen C, Farrer LA (2005) Complement factor h polymorphism and age-related macular degeneration. Science 308:421–424
17. Ekmekci H, Sonmez H, Ekmecki OB, Ozturk Z, Domanic N (2002) Plasma vitronectin levels in patients with coronary atherosclerosis are increased and correlate with extent of disease. J Thromb Thrombolysis 14:221–225

18. Grossniklaus HE, Green WR (1998) Histopathologic and ultrastructural findings of surgically excised choroidal neovascularization. Submacular surgery trials research group. Arch Opthalmol 116:745–749
19. Hagemann, GS; Mullins RF, Russell SR, Johnson LV, Anderson DH (1999) Vitronectin is a constituent of ocular drusen and the vitronectin gene is expressed inhuman retinal pigmented epithelial cells. FASEB J 13:477–484
20. Hageman GS, Luthert PJ, Victor Chong NH, Johnson LV, Anderson DH, Mullins RF (2001) An integrated hypothesis that considers drusen as biomarkers of immune-mediated processes at the RPE-Bruch's membrane interface in aging and age-related macular degeneration. Prog Retin Eye Res 20:705–732
21. Hageman GS, Anderson DH, Johnson LV, Hancox LS, Taiber AJ, Hardisty LI et al (2005) A common haplotype in the complement regulatory gene factor H (HF1/CFH) predisposes individuals to age-related macular degeneration. Proc Natl Acad Sci USA 102:7227–7232
22. Haines JL, Hauser MA, Schmidt S, Scott WK, Olson LM, Galins P, Spencer KL, Kwan Sy, Noureddine M, Gilbert JR, Schnetz-Boutaud N, Agarwal A, Postel EA, Pericak-Vance MA (2005) Complement Factor H variant increases the risk of age-related macular degeneration. Science 308:419–421
23. Hermans P, Lommatzsch A, Bornfeld N, Pauleikhoff D (2003) Angiographic-histological correlation of late exudative age-related macular degeneration. Ophthalmologe 100:378–383
24. Holz FG, Sheraidah G, Pauleikhoff D, Bird AC (1994) Analysis of lipid deposits extracted from human macular and peripheral bruch's mmbrane. Arch Ophthalmol 112:402–406
25. Johnson LV, Leitner WP, Staples MK, Anderson DH (2001) Complement activation and inflammatory processes in drusen formation and age-related macular degeneration. Exp Eye Res 73:887–896
26. Kadonosono K, Yazama F, Itoh N, Sawada H, Ohno S (1999) Expression of matrix metalloproteinase-7 in choroidal neovascular membranes in age-related macular degeneration. Am J Ophthalmol 128:382–384
27. Kini MM, Leibowitz HM, Colton T, Nickerson RJ, Ganley J, Dawber TR (1978) Prevalence of senile cataract, diabetic retinopathy, senile macular degeneration, and open-angle glaucoma in the Framingham Eye Study. Am J Ophthalmol 85:28–34
28. Klein RJ, Zeis C, Chew EY, Tsai J-Y, Sackler RS, Haynes C, Henning AK, SanGiovanni JP, Mane SM, Mayne ST, Bracken MB, Ferris FL, Ott J, Barnstable C, Hoh J (2005) Complement factor h polymorphism in age-related macular degeneration. Science 308:385–389
29. Kliffen M, van der Schaft TL, Mooy CM, de Jong, PTVM (1997) morphologic changes in age-related maculopathy. Microsc Res Tech 36:106–122
30. Knupp C, Amin SZ, Munro PMG, Luthert PJ, Squire JM (2002) Collagen VI assemblies in age-related macular degeneration. J Struct Biol 139:181–189
31. Kvanta A, Shen WY, Sarman S, Seregard S, Steen B, Rakoczy E (2000) Matrix metalloproteinase (MMP) expression in experimental choroidal neovascularization. Curr Eye Res 21:684–690
32. Lafaut BA, Aisenbrey S, van den Broecke C, Di Tizio F, Bartz-Schmidt KU (2001) Clinicopathological correlation in exudative age-related macular degeneration: recurrent choroidal neovascularisation. Graefes Arch Clin Exp Ophthalmol 239:5–11
33. Lambert V, Wielockx B, Munaut C, Galopin C, Jost M, Itoh T, Werb Z, Baker A, Libert C, Krell HW, Foidart JM, Noel A, Rakic JM (2003) MMP-2 and MMP-9 synergize in promoting choroidal neovascularization. FASEB J 17:2290–2292
34. Lopez PF, Grossniklaus HE, Lambert HM, Aaberg TM, Capone A Jr, Sternberg P Jr, L'Hernault N (1991) Pathologic features of surgically excised subretinal neovascular membranes in age-related macular degeneration. Am J Opthalmol 112:647–656
35. Loeffler KU, Lee WR (1986) Basal linear deposits in the human macula. Graefes Arch Clin Exp Ophthalmol 224:493–501
36. Marshall GE, Konstas AG, Reid GG, Edwards JG, Lee WR (1994) Collagens in the aged human macula. Graefes Arch Clin Exp Ophthalmol 232:133–140
37. Pauleikhoff D, Harper A, Marshall J, Bird AC (1990) Aging changes in Bruch's membrane. a histochemical and morphologic study. Ophthalmology 97:171–178
38. Pauleikhoff D, Sheraidah G, Marshall J, Bird AC, Wessing A (1994) Biochemische und histochemische Analyse altersabhängiger Lipidablagerungen in der Bruchschen Membran. Ophthalmologe 91:730–734
39. Pauleikhoff D, Zuels S, Sheraidah GS, Marshall J, Wessing A, Bird AC (1992) Correlation between biochemical composition and fluorescein binding of deposits in Bruch's membrane. Ophthalmology 99:1548–1553
40. Pickering MC, Cook HT, Warren J, Bygrave AE, Moss J, Walport MJ, Botto M (2002) Uncontrolled C3 activation causes membranoproliferative glomerulonephritis in mice deficient in complement factor H. Nat Genet 31:424–428
41. Reynolds ES (1963) The use of lead citrate at high pH as an electron opaque stain in electron microscopy. J Cell Biol 17:208–212
42. Sarks SH (1976) Ageing and degeneration in the macular region: a clinico-pathological study. Br J Ophthalmol 60:324–341
43. Sarks JP, Sarks SH, Killingsworth MC (1988) Evolution of geographic atrophy of the retinal pigment epithelium. Eye 2:552–577
44. Sarks SH, Cherepanoff S, Killingsworth MC, Sarks JP (2007) Relationship of basal laminar deposits and membranous debris to the clinical presentation of early age-related macular degeneration. Invest Ophthalmol Vis Sci 48:968–977
45. Curcio CA, Presley JB, Malek G, Medeiros NE, Avery DV, Kruth HS (2005) Esterified and unesterified cholesterol in drusen and basal deposits of eyes with age-related maculopathy. Exp Eye Res 81:731–741
46. Scott JE, Dorling J (1965) Differential staining of acid glycosaminoglycans (mucopolysaccharides) by alcian blue in salt solution. Histochemie 5:221–233
47. Schlingemann RO (2004) Role of growth factors and the wound healing response in age-related macular degeneration. Graefes Arch Clin Exp Ophthalmol 242:91–101
48. Steen B, Sejersen S, Berglin L, Seregard S, Kvanta A (1998) Matrix metalloproteinases and metalloproteinase inhibitors in choroidal neovascular membranes. Invest Ophthalmol Vis Sci 39:2194–2200
49. Van der Schaft TL, Mooy CM, de Bruijn WC, Bosman FT, de Jong PT (1994) Immunohistochemical light and electron microscopy of basal laminar deposit. Graefes Arch Clin Exp Ophthalmol 232:40–46
50. Zarbin MA (2004) Current concepts in the pathogenesis of age-related macular degeneration. Arch Ophthalmol 122:598–614 (Review)